J Mater Sci (2011) 46:2345–2349
DOI 10.1007/s10853-010-5080-5

Study on the sintering mechanism of KNN-based lead-free piezoelectric ceramics

Xuming Pang · Jinhao Qiu · Kongjun Zhu · Jun Luo

Received: 8 June 2010 / Accepted: 12 November 2010 / Published online: 3 December 2010
© Springer Science+Business Media, LLC 2010

Abstract The sintering process and mechanism of (K, Na, Li) (Nb, Ta, Sb)O_3 (KNLNTS) solid solution were investigated. The results show that the KNLNTS forms via the reaction of A_2CO_3(A: K,Na,Li) and B_2O_5(B: Nb,Ta,Sb) at 400–800 °C. The kinetics for the formation of KNLNTS during solid-state reaction is investigated using an isothermal method. Based on the reaction kinetic isothermal analysis, KNLNTS formation is corroborated as being controlled by diffusion mechanism. It has been found that sintering densification occurs within a narrow temperature range, and the density decreases apparently when the sintering temperature slightly exceeds the optimal one. Abnormal grain growth tends to occur after reaching the maximum density and get intensified with increasing temperature. The effect of sintering temperature and time on the shrinkage of powder compacts during sintering were studied. The sintering process in the KNLNTS solid solutions may be explained by the grain boundary diffusion model inferring from the shrinkage rate of about 0.3.

Introduction

Lead oxide-based piezoelectric ceramics including lead zirconate titanate (PZT) have been widely used for various applications such as piezoelectric transformers, ultrasonic motors, actuators, sensors, filters, and resonators, because of their excellent piezoelectric properties. However, owing to the toxicity of lead oxide that is largely used during the production process, there is an increasing demand to replace them with lead-free alternatives, among which lead-free alkali niobate ceramics based on (K, Na)NbO_3 (abbreviated as KNN) are the most promising[1–12].Their piezoelectric properties could be improved by introducing dopant such as Li,Ta, and Sb into the A and B sites of ABO_3 in pervoskite-structured KNN systems[1–3]. Recently, Saito et al. obtained an even high d_{33} of about 300 and 416 pC/N in the $(Na_{0.52}K_{0.44}Li_{0.04})$ $(Nb_{0.86}Ta_{0.10}Sb_{0.04})O_3$ ceramic and the textured one, respectively[1]. Thereafter, (K, Na, Li) (Nb, Ta, Sb)O_3 piezoelectric ceramics attracted researchers′ attention [13, 14].

The sintering process and mechanism of (K, Na, Li) (Nb, Ta, Sb)O_3 (KNLNTS) solid solution, however, have not been reported up to date. It is well known that it is difficult to get a dense KNN ceramic specimen by the normal sintering method, and many efforts have been made to fabricate it. In order to optimize the sintering process, the investigation was undertaken to study the sintering process in KNLNTS solid solutions and to discuss the sintering mechanism of KNLNTS.

Experimental procedure

The ceramics with the composition of $(K_{0.4425}Na_{0.52}Li_{0.0375})$ $(Nb_{0.8925}Ta_{0.0375}Sb_{0.07})O_3$ (KNLNTS) were manufactured by a solid-state reaction method. Na_2CO_3 (99.8%), K_2CO_3 (99.0%), Li_2CO_3 (98%), Nb_2O_5 (99.5%), Ta_2O_5 (99.9%), and Sb_2O_5 (99.5%) were used as raw materials. In order to remove absorbed water, the raw materials were dried at 110 °C for 4 h. The powders were weighed and mixed well in alcohol by ball milling for 12 h. Then, the calcination was conducted at 900 °C for 5 h. The calcined mixture was ball-milled in alcohol again for 12 h.

X. Pang · J. Qiu (✉) · K. Zhu · J. Luo
The Aeronautical Key Laboratory for Smart Materials and Structures, Nanjing University of Aeronautics and Astronautics, Nanjing 210016, Jiangsu, People's Republic of China
e-mail: qiu@nuaa.edu.cn

After drying, the dried powders were pressed into bars of 15 mm in diameter and 6 mm in thickness for the shrinkage experiments then sintered in air at 1040–1140 °C. The shrinkage was determined by measuring the distance between the two surfaces of the bar.

The crystal phase of the premixed powders by heating at different temperatures were determined using X-ray diffraction (XRD) analysis with CuKα radiation (D8 Advance) at a scan speed of 4°/min and a step width of 0.02°. Thermal analysis DSC/TG was carried out using a Netzsch STA 449C thermal analyzer, in which the samples were heated at a rate of 15 °C/min from room temperature to 1000 °C. The microstructure of the bulk was examined using scanning electron microscopy (FEI Quanta 200). The density of the sintered bulks was measured by the Archimedes method.

Results and discussion

Figure 1 shows the DSC-TG result for a sintering process. The endothermic peaks at 75 and 99 °C on the heating curve are observed, respectively. Obviously, the endothermic peaks correspond to the evaporation of alcohol and water at 75 and 99 °C, respectively. The weight loss also corresponds to the evaporation of alcohol and water before 100 °C. The exothermal process in the differential scanning calorimetry curves is displayed at 400–800 °C, which indicates that some chemical reactions occur.

Figure 2 shows the XRD patterns of powders sintered from various temperatures. The XRD analysis was performed at room temperature by interrupting sintering at various stages. Figure 3 shows the variation of the selected XRD peaks of the major constituents involved in the sintering of the raw material powders. The relative intensity in the plot is defined as the height of peak of interest divided by the height of the certain peak observed in an XRD scan. As such, the latter relative intensity does not necessarily provide a legitimate basis for quantitative comparison of peak intensities. It does, however, provide a quick means of observing the variation of the amount of a phase during sintering.

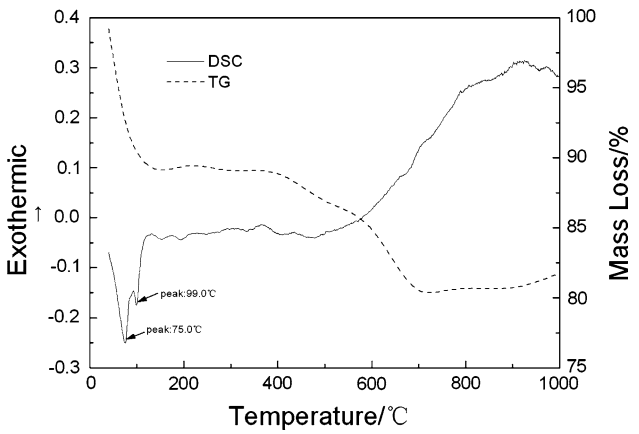

Fig. 1 DSC and TG curve of raw material powder for KNLNTS

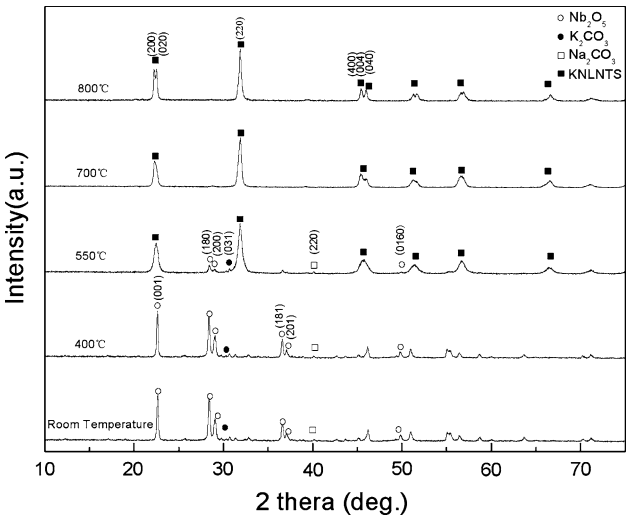

Fig. 2 XRD patterns of powders from various temperatures

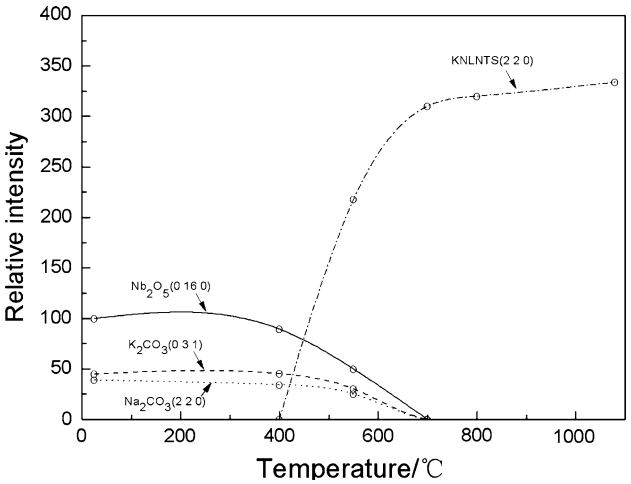

Fig. 3 RT-XRD peak intensities of the phases in KNLNTS as a function of sintering temperature

Relative intensities of X-ray diffraction of main phases of ceramic versus sintering temperature are shown in Fig 3. The intensity of Nb_2O_5 (0 16 0) at room temperature is used as a benchmark (namely, the Nb_2O_5 (0 16 0) intensity was defined as 100), and the intensity of K_2CO_3 (031),Na_2CO_3 (220),Nb_2O_5 (0 16 0), and KNLNTS (220) at different temperatures could gain by comparing with the intensity of Nb_2O_5 (0 16 0) at room temperature (Because of the thimbleful amount of Li_2CO_3,Ta_2O_5,and Sb_2O_5, their diffraction peaks were hardly observed).

The anterior results suggest that KNLNTS forms above 400 °C via the reaction of A_2CO_3 (A: K, Na, Li) and B_2O_5 (B: Nb, Ta, Sb), giving rise to the exothermic process at

400 °C in Fig. 1. The relative intensities of X-ray diffraction of each phase are in direct proportion with the amount. The amount of KNLNTS gradually increases, while the amount of A_2CO_3 and B_2O_5 reduces with the temperature increasing. When the temperature reaches 700 °C, a greater amount of A_2CO_3 have reacted with B_2O_5, and so little amount of carbonates are hardly observed by X-ray diffraction. The reaction completely comes to a finish at 800 °C. The TG curve of raw material powders for KNLNTS is shown in Fig 1. The weight loss between 400 and 700 °C indicates that gas generates during the reaction of A_2CO_3 and B_2O_5. Therefore, the reaction is at 400–800 °C as follows:

$$A_2CO_3 + B_2O_5 = ABO_3 + CO_2 \uparrow . \quad (1)$$

Here, A represents K, Na, Li; and B represents Nb,Ta, Sb.

The rate of the perovskite phase formation (wt% perovskite) is considered at 700 °C and at various dwell times. These relative amounts of perovskite, A_2CO_3, and B_2O_5 phases, are approximated by mensurating the amount of carbon dioxide and using the equation (1). The percentage increases of the perovskite phase formation of the calcined powders, resulting from the calcinations process at 700 °C and various dwell times, is shown in Table 1.

Accordingly, the Johnson–Mehl–Avrami, or JMA equation is used in this study. This equation is found appropriate for describing a wide variety of isothermal solid-state transformations [15, 16]. It is used to study the kinetics of the reaction and mechanism involving nucleation and grain growth, and has the general form of

$$\alpha = 1 - \exp(-\gamma t^m) \quad (2)$$

where α is the percentage of the perovskite phase formed, γ is the reaction rate, t is the reaction time, and m is a constant which will vary with the system geometry. With proper linearization process, Eq. (2) can be written as

$$\ln[-\ln(1-\alpha)] = \ln(\gamma) + m\ln(t) \quad (3)$$

According to the values of m in Eq. (3), the solid-state reactions can be divided into three groups: a diffusion mechanism for $m = 0.52$–0.62, a first-order or phase boundary mechanism for $m = 1.0$–1.24, and a nucleation or growth mechanism for $m = 2.0$–3.0 [17]. By substituting the fraction of the perovskite phase, given in Table 1, into Eq. (3), one can make a plot of the regression lines of Eq. (3), as shown in Fig. 4. The value of m at 700 °C is estimated to be 0.52. This indicates that the reaction of solid solution formation is diffusion-controlled process.

Table 1 Fraction of perovskite phase formed as a function of dwell time

Dwell time(min)	5	15	30	45
%Perovskite	0.774	0.818	0.975	0.980

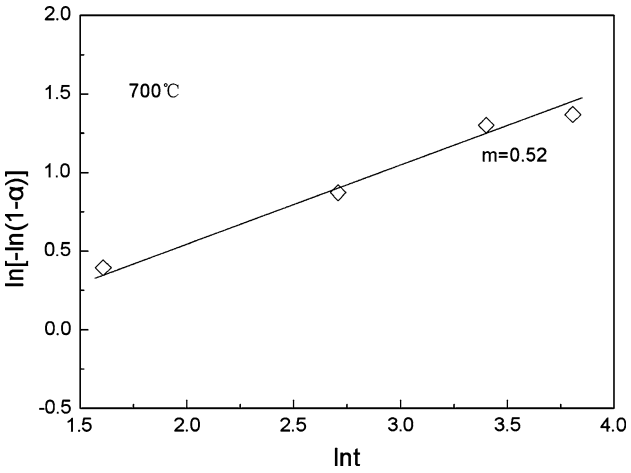

Fig. 4 Plot of $\ln((-\ln(1-\alpha))$ versus $\ln(t)$ for the reaction process

Figure 5 shows SEM micrographs of KNLNTS samples. As shown in Fig. 5(a), the grains are still within the submicron range even when sintered at 1100 °C. When the sintering temperature is increased to 1120 °C, the microstructure becomes denser, and the grains grow much larger. It is easy to distinguish large grains which grow significantly and result in a bimodal distribution containing coarse and faceted grains; many fine grains are distributed at the boundaries of coarse grains. Such a microstructural feature is maintained in the sample sintered at 1130 °C, as shown in Fig. 5(c). However, some abnormal tetragonal grains and square grains have grown up to 4 μm. It can be seen from Fig. 5(d) that many distinct pores exist in the grain boundary of KNLNTS ceramics sintered at 1140 °C, and the tetragonality of grain decreases. Because the solidus temperature of KNN is near 1140 °C [18], it indicates that the liquid phase is formed, which makes sharp corner of grains dissolve. This result explains that the KNLNTS grains of the sample sintered at 1120 °C grow sufficiently.

Figure 6 shows the change in the sintered densities of the KNLNTS ceramics with sintering temperature. Note that the sintering temperature is changed within a narrow range, but the density changes significantly at 1100–1140 °C. The densities of the KNLNTS samples increase from 4.31 to 4.52 g/cm^3 when the sintering temperature is increased from 1100 to 1120 °C, but it tends to decrease when the temperature is further increased. These results also confirm that the optimum sintering temperature of KNLNTS ceramics is 1120 °C.

The effect of sintering temperature and time on the shrinkage of powder compacts during sintering are

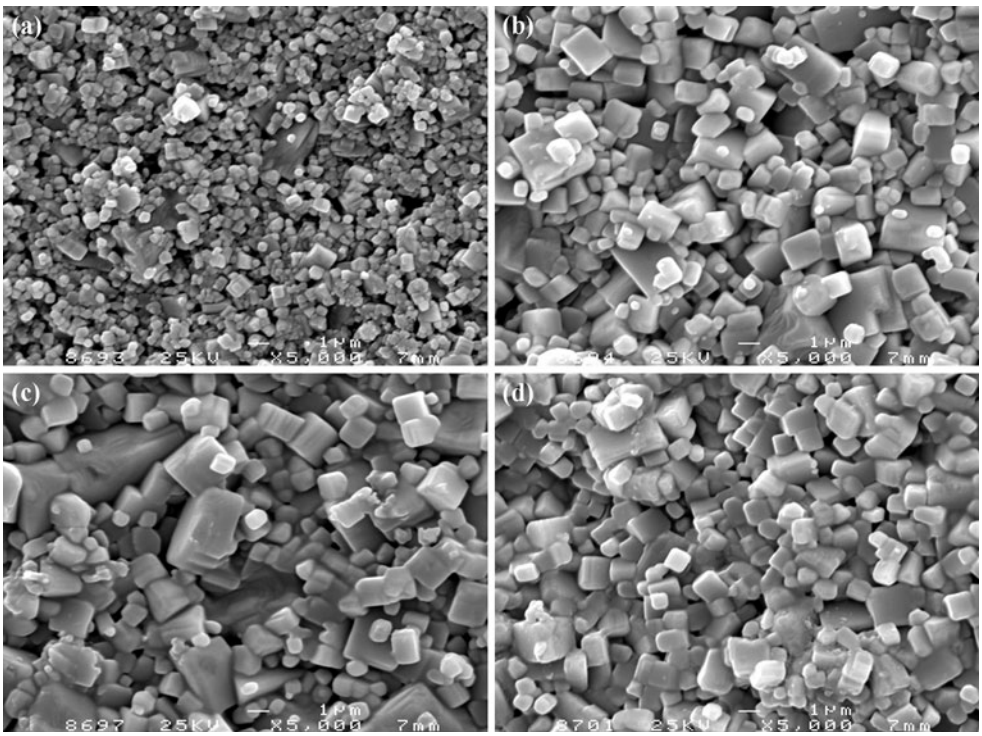

Fig. 5 SEM micrographs of KNLNST sintered at **a** 1100 °C, **b**1120 °C, **c**1130 °C, **d**1140 °C

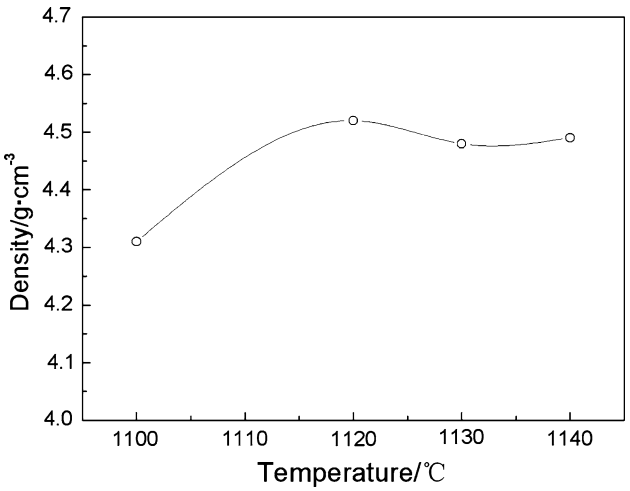

Fig. 6 Density change of KNLNTS ceramics with sintering temperature

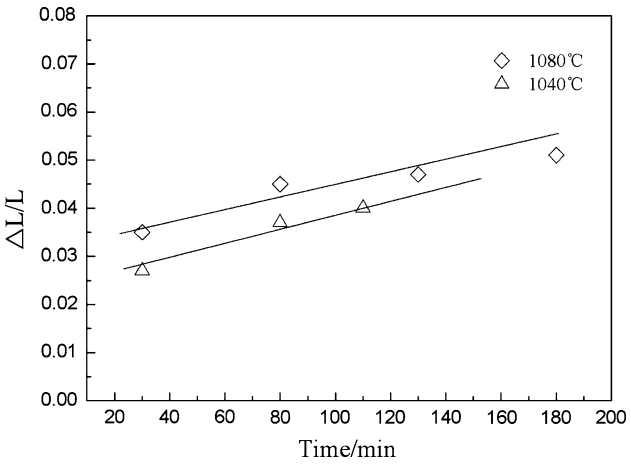

Fig. 7 The relationship between shrinkage and time

examined.The isothermal shrinkage of the powder compact is shown against time in Fig. 7, where Lo and L = Lo− △L are the thicknesses of the bar before and after sintering, respectively. It is obvious that the linear shrinkage occurs at every temperature. The slopes of these two lines are about 0.3.

The theoretical approach of sintering by use of two spheres or a sphere and a plate were done by Kingery and Berg, Coble, and Lynn Johnson and Cutler Ivan [19–23]. They show that the densification occurs by the neck growth and for the diffusion model of sintering the linear shrinkage of the sphere is described as

$$\left(\frac{\Delta L}{L_0}\right) = B\left(\frac{D\gamma\delta^3}{R^m KT}t\right)^{\frac{1}{p}}. \quad (4)$$

where B is numerical constant; R is initial radius of sphere; D is diffusion constant; γ is surface energy; δ is atomic distance; t is time; K is boltzmann constant, p and m are constants depending on the sintering mechanism.

The value of 1/p is about 0.3 which corresponds to the grain boundary diffusion model [19–23]. Therefore, the

sintering mechanism of KNLNTS may be explained by the grain boundary diffusion model inferring from the shrinkage rate of about 0.3. Based on the grain boundary diffusion model, the substance transferred from other part results in the neck growth; in other words, the vacancies transferred from interface to grain boundary disappear. Thus, the densification could gradually complete by the neck growth in the KNN system.

Conclusions

In summary, the sintering process and mechanism of (K, Na, Li) (Nb, Ta, Sb)O_3 (KNLNTS) solid solution were investigated. It is determined that the KNLNTS forms via the reaction of $A_2CO_3 + B_2O_5 = ABO_3 + CO_2\uparrow$ at 400–800 °C. The reaction mechanism and kinetic analysis for the formation of KNLNTS are investigated. The formation of KNLNTS is confirmed to be governed by a diffusion controlled mechanism via reaction kinetic isothermal analysis. It has been found that sintering densification occurs within a narrow temperature range, and the density decreases apparently when the sintering temperature slightly exceeds the optimal one. Abnormal grain growth tends to occur after reaching the maximum density and get intensified with increasing temperature. Effect of sintering temperature and time on the shrinkage of powder compacts during sintering were studied. The sintering process in the KNLNTS solid solutions may be explained by the grain boundary diffusion model.

Acknowledgements This study was supported by the National Nature Science Foundation of China (NSFC no. 50872053), the Cultivation Fund of the Key Scientific and Technical Innovation Project of Ministry of Education of China (no.707031), and Program for Changjiang Scholars and Innovative Research Team in University under Grant No. IRT0906.

References

1. Saito Y, Takkao H, Tani T, Nonoyama T, Takatori K, Hommal T, Nagaya T, Nakamura M (2004) Nature 84:432
2. Chang YF, Yang ZP, Hou YT, Liu ZH, Wang ZL (2007) Appl Phys Lett 90:232905
3. Saito Y, Takkao H (2006) Ferroelectrics 338:17
4. Yoo JH, Yoo KH, Lee YW, Suh SS, Kim JS, Yoo CS (2000) Jpn. J Appl Phys 39:2680
5. Li JF, Wang K, Zhang BP, Zhang LM (2006) J Am Ceram Soc 89:706
6. Wu JG, Xiao DQ, Wang YY, Zhu JG, Wu L, Jiang YH (2007) Appl Phys Lett 91:132914
7. Zhao P, Zhang BP, Li JF (2007) Appl Phys Lett 90:242909
8. Wang K, Li JF (2007) Appl Phys Lett 91:262902
9. Zhao P, Zhang BP, Li JF (2007) Appl Phys Lett 91:172901
10. Zhao P, Zhang BP, Li JF (2007) Scripta Mater 58:429
11. Zhen YH, Li JF (2006) J Am Ceram Soc 89:3369
12. Zhang BP, Li JF, Wang K, Zhang HL (2006) J Am Ceram Soc 89:160
13. Zuo RZ, Fu J, Lv DY (2009) J Am Ceram Soc 92:183
14. Fu J, Zuo RZ, Wang XH (2009) J Phys D Appl Phys 42:0212006
15. Sheibani S, Ataie A, Heshmati-Manesh S (2008) J Alloys Compd 455:447
16. Yan ZJ, Dang SE, Wang XH, Lian PX (2008) Trans Nonferrous Met Soc China 18:138
17. Seo KW, Oh JK (2008) J Ceram Soc Jpn 108:691
18. Ringgaard E, Wurlitzer T (2005) J Eer Ceram Soc 25:2701
19. Kingery WD, Berg M (1955) J Appl Phys 26:1205
20. Lynn Johnson D, Cutler Ivan (1963) J Am Ceram Soc 46:541
21. Coble RL (1958) J Am Ceram Soc 41:55
22. Coble RL (1961) J Appl Phys 32:787
23. Lynn Johnson D, Cutler Ivan (1963) J Am Ceram Soc 46:545